International Journal of Bifurcation and Chaos, Vol. 33, No. 10 (2023) 2350122 (11 pages)

DOI: 10.1142/S0218127423501225

Similar Master Stability Functions for Different Coupling Schemes in Basic Chaotic Systems

Zahra Dayani, Fatemeh Parastesh* and Sajad Jafari†,‡
Department of Biomedical Engineering,
Amirkabir University of Technology (Tehran Polytechnic), Iran
**Centre for Nonlinear Systems, Chennai Institute of Technology, Chennai, India*
†*Health Technology Research Institute,*
Amirkabir University of Technology (Tehran Polytechnic), Iran
‡*sajadjafari83@gmail.com*

Eckehard Schöll
Institut für Theoretische Physik, Technische Universität Berlin,
Hardenbergstrasse 36, 10623 Berlin, Germany
Bernstein Center for Computational Neuroscience Berlin,
Humboldt-Universität, 10115 Berlin, Germany
Potsdam Institute for Climate Impact Research,
Telegrafenberg A 31, 14473 Potsdam, Germany

Jürgen Kurths
Potsdam Institute for Climate Impact Research,
Telegrafenberg A 31, 14473 Potsdam, Germany
Department of Physics, Humboldt University Berlin,
Berlin 12489, Germany

Julien Clinton Sprott
Department of Physics, University of Wisconsin–Madison,
Madison, WI 53706, USA

Received July 18, 2023

Synchronization is a prominent phenomenon in coupled chaotic systems. The master stability function (MSF) is an approach that offers the prerequisites for the stability of complete synchronization, which is dependent on the coupling configuration. In this paper, some basic chaotic systems with the general form of the Sprott-A, Sprott-B, Sprott-D, Sprott-F, Sprott-G, Sprott-O, and Jerk systems are considered. For each system, their parametric form is designed, and constraints required to have similar MSFs in different coupling schemes are determined. Then, the parameters of the designed chaotic systems are found through an exhaustive computer search seeking chaotic solutions. The simplest cases found in this way are introduced, and similar synchronization patterns are confirmed numerically.

Keywords: Synchronization; master stability function; simple chaotic system.

‡Author for correspondence

1. Introduction

Coupled oscillatory systems represent a dynamical network with manifold characteristics [Boccaletti *et al.*, 2006]. Synchronization is among the most significant ones [Pikovsky *et al.*, 2002; Lü *et al.*, 2004]. The intrinsic dynamics of the single systems in this phenomenon is modified to maintain the same trajectory as they evolve over time [Belykh *et al.*, 2005]. Synchronization may occur as a result of proper coupling, feedback, or external stimulation [Rafikov & Balthazar, 2008; Dahms *et al.*, 2012; Franović *et al.*, 2014; Zhou *et al.*, 2021; Sawicki *et al.*, 2022]. Applications for synchronization have been discussed in a variety of fields, including physics, biology, engineering, and social sciences [Moskalenko *et al.*, 2013; Wang *et al.*, 2018; Couzin, 2018; Rakshit *et al.*, 2018; Parastesh *et al.*, 2022].

Over the past two decades, much research has been done on synchronizing chaotic systems [Boccaletti *et al.*, 2002]. This interest is derived from using chaotic systems' synchronization in control theory, neurology, secure communication, and cryptography [Antonik *et al.*, 2018; Chen *et al.*, 2019; Tang *et al.*, 2021; Wang *et al.*, 2009]. Different types of chaos synchronization exist, including full, generalized, phase, and lag synchronization [Rosenblum *et al.*, 1996, 1997; Franović *et al.*, 2012; Rakshit & Ghosh, 2020; Frolov & Hramov, 2021; Amritkar & Rangarajan, 2009]. Complete (full) synchronization happens when two or more initially different systems arrive at the same attractor with similar temporal behavior. One of the crucial issues in this field is examining the stability of synchronization [Pecora & Carroll, 2015; Li & Chen, 2006]. The ability of a network to stay with the dynamics on the synchronization manifold despite a variety of disturbances and disruptions is referred to as synchronization stability.

A well-known method for examining local stability of synchronization in complicated dynamical systems is the master stability function (MSF) [Pecora & Carroll, 1990, 1998]. This technique determines the stability of the synchronization manifold for any coupling topology by calculating the largest Lyapunov exponent of the synchronized solution as a function of a formal complex parameter λ, i.e. the MSF. If this function is negative for any eigenvalue of the coupling (adjacency) matrix substituted for λ, then the synchronization manifold is stable. The MSF offers insights into the dynamic behavior of the network and can assist in achieving performance with improved synchronization [Faghani *et al.*, 2020]. The MSF approach is described in the Appendix.

Symmetries in the system's equations provide distinctive characteristics, such as equivalent synchronization dynamics, obtained by computing MSFs. Chaotic circulant systems with cyclic symmetry are basic examples for this [Panahi *et al.*, 2021]. A three-dimensional circulant system is defined as,

$$\begin{aligned} \dot{x} &= f(x, y, z), \\ \dot{y} &= f(y, z, x), \\ \dot{z} &= f(z, x, y). \end{aligned} \tag{1}$$

In these systems, there are identical MSFs for some coupling functions due to the symmetries. For example, by considering $f(x, y, z) = y^2 - z$, a chaotic circulant system is obtained with the following equations [Panahi *et al.*, 2021],

$$\begin{aligned} \dot{x} &= y^2 - z, \\ \dot{y} &= z^2 - x, \\ \dot{z} &= x^2 - y. \end{aligned} \tag{2}$$

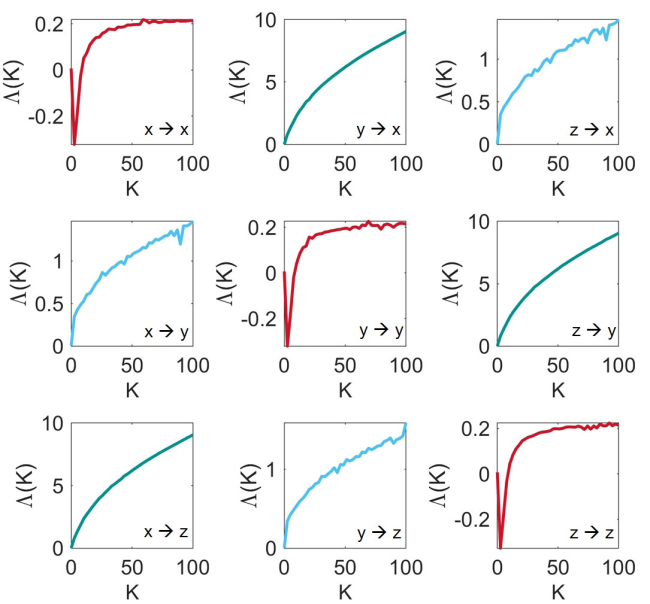

Fig. 1. Master stability functions ($\Lambda(K)$) of the circulant system in Eq. (2) in dependence on K for different coupling schemes. This system has only three distinct MSF curves. The notations represent the coupling configuration where e.g. in $x \rightarrow y$ coupling, the coupling is defined in the x state variables and added to the dynamic equation of the y state variables.

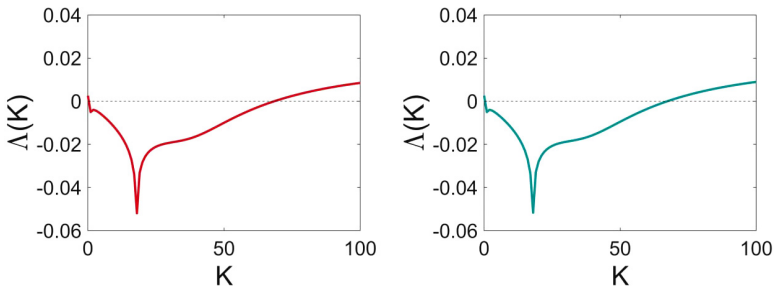

Fig. 2. Master stability functions ($\Lambda(K)$) of the jerk system [Eq. (4)] in dependence on K for $y \to y$ and $z \to z$ couplings.

On the other hand, a network of coupled oscillators can be described as

$$\dot{X}_i = F(X_i) - \sigma \sum_{j=1}^{N} L_{ij} H(X_j), \tag{3}$$

where $X_i = (x, y, z)$ is a three-dimensional state vector, F defines the local nonlinear oscillator dynamics, $i = 1, \ldots, N$ denotes the index of the network nodes and σ shows the overall coupling strength. The $N \times N$ matrix L is the Laplacian matrix of the network, and $H(X) = hX$ defines the coupling scheme (more details are given in the Appendix).

The MSFs $\Lambda(K)$, where $K = \sigma\lambda$ is the rescaled coupling strength, of this system for all single-variable coupling schemes are shown in Fig. 1. The notation $x \to y$ coupling represents that the coupling is defined in x state variables and added to the dynamic equation for the y state variables. It follows from the circulant symmetry that this system has equivalent MSF curves in $x \to x$, $y \to y$, $z \to z$, also in $x \to y$, $y \to z$, $z \to x$ and in $x \to z$, $y \to x$, $z \to y$ couplings. Therefore, there is no difference in synchronization when coupled in $x \to x$ or $y \to y$ or $z \to z$; also for the two other symmetry groups.

Another nontrivial example is a certain type of chaotic system, called the jerk system. It was recently demonstrated by Mirzaei *et al.* [2022] that specific jerk systems can have identical MSFs in velocity coupling (y) and acceleration coupling (z). They discovered that jerk systems, in which the jerk equation is independent of acceleration, have identical MSFs in two coupling configurations $y \to y$ and $z \to z$. An example of these systems is as follows,

$$\begin{aligned} \dot{x} &= y, \\ \dot{y} &= z, \\ \dot{z} &= -8y + |x| - 1. \end{aligned} \tag{4}$$

As mentioned, this system has the same MSF curves in $y \to y$, $z \to z$ coupling configurations, which are shown in Fig. 2.

As a result of the findings discussed above, we look for basic 3D chaotic systems with the same MSF curves in various coupling configurations in this paper. To achieve this, some well-known chaotic systems are taken into consideration, and their third equation is substituted with a general parametric quadratic equation. Different forms of parametric equations that lead to having identical MSFs in various couplings are then determined by using the equations relating to MSF. Consequently, a systematic numerical search for chaotic solutions enables us to identify the coefficients of the designed chaotic systems.

2. The Design Method

Some basic chaotic systems are considered, including Sprott-A, Sprott-B, Sprott-D, Sprott-F, Sprott-G, Sprott-O, and a jerk system [Sprott, 1994]. The third equation of these systems is replaced by a general parametric equation with constant, linear and quadratic terms as follows,

$$\begin{aligned} \dot{x} &= f_1(x, y, z), \\ \dot{y} &= f_2(x, y, z), \\ \dot{z} &= a_1 x + a_2 y + a_3 z + a_4 x^2 + a_5 y^2 + a_6 z^2 \\ &\quad + a_7 xy + a_8 xz + a_9 yz + a_{10}. \end{aligned} \tag{5}$$

To find chaotic systems with identical MSFs for each case, firstly, some constraints should be derived. Then, the parameters that meet these conditions should be found. Using a systematic search, the coefficients of the parametric equations are computed so that chaotic dynamics exist. In the following, the procedure for finding desired systems is explained. As an example, the Sprott-A system is considered.

The original Sprott-A system is defined as,

$$\dot{x} = y, \quad \dot{y} = -x + yz, \quad \dot{z} = 1 - y^2. \tag{6}$$

First of all, the third equation is substituted by a general parametric equation as,

$$\begin{aligned} \dot{x} &= y, \\ \dot{y} &= -x + yz, \\ \dot{z} &= a_1 x + a_2 y + a_3 z + a_4 x^2 + a_5 y^2 + a_6 z^2 \\ &\quad + a_7 xy + a_8 xz + a_9 yz + a_{10} \end{aligned} \tag{7}$$

leading to the Jacobian matrix,

$$DF = \begin{bmatrix} 0 & 1 & 0 \\ -1 & z & y \\ f_x & f_y & f_z \end{bmatrix}, \tag{8}$$

where f_x, f_y, f_z are the partial derivatives of the polynomial equation in (6) as,

$$\begin{aligned} f_x &= a_1 + 2a_4 x + a_7 y + a_8 z, \\ f_y &= a_2 + 2a_5 y + a_7 x + a_9 z, \\ f_z &= a_3 + 2a_6 z + a_8 x + a_9 y. \end{aligned} \tag{9}$$

As explained in the Appendix, the MSF is the largest Lyapunov exponent of Eq. (A.3). Since the Lyapunov exponents are related to the temporally averaged normalized dynamic eigenvalues Λ, we compute the eigenvalues of Eq. (A.3) as follows:

$$\mathrm{Det}(\Lambda I - (DF - Kh)) = 0, \tag{10}$$

where I is the unity matrix. Next, the eigenvalues are calculated for all single-variable couplings. The resultant equations for the dynamic eigenvalues of the Sprott-A system are obtained as,

$$\begin{aligned} x \to x: &\quad \Lambda^3 + (-f_z + k - z)\Lambda^2 + (1 - f_z k - f_y y + f_z z - kz)\Lambda - f_z - f_x y - f_y ky + f_z kz = 0, \\ y \to x: &\quad \Lambda^3 + (-f_z - z)\Lambda^2 + (1 - k - f_y y + f_z z)\Lambda - f_z + f_z k - f_x y + f_x ky = 0, \\ z \to x: &\quad \Lambda^3 + (-f_z - z)\Lambda^2 + (1 + f_x k - f_y y + f_z z)\Lambda - f_z - f_y k - f_x y - f_x kz = 0, \\ x \to y: &\quad \Lambda^3 + (-f_z - z)\Lambda^2 + (1 + k - f_y y + f_z z)\Lambda - f_z - f_z k - f_x y = 0, \end{aligned}$$

Table 1. Parametric systems with identical MSFs based on Sprott-A system [Eq. (7)] ($m \to n$ coupling means that m state variables affect the dynamics of the n state variables).

	System	Parameters	Couplings with Identical MSF
1	$\dot{x} = y$	$a_1 = -a_2$	$y \to x$
	$\dot{y} = -x + yz$	$2a_3 + a_5 = 1$	$z \to x$
	$\dot{z} = -x + a_1 y + a_2 z + a_3 y^2 + a_4 z^2 + a_5 yz + a_6$	$2a_4 + a_5 = 1$	
2	$\dot{x} = y$	$a_1 = a_2$	$z \to x$
	$\dot{y} = -x + yz$	$a_5 = 2a_3$	$x \to y$
	$\dot{z} = x + a_1 y + a_2 z + a_3 y^2 + a_4 z^2 + a_5 yz + a_6$	$2a_4 - a_5 = 1$	
3	$\dot{x} = y$	$a_1 = -a_2$	$x \to y$
	$\dot{y} = -x + yz$	$a_3 = -0.5a_5$	$z \to y$
	$\dot{z} = a_1 x + y + a_2 z + a_3 x^2 + a_4 z^2 + a_5 xz + a_6$	$a_4 = -0.5a_5$	
4	$\dot{x} = y$	No constraint	$z \to x$
	$\dot{y} = -x + yz$		$x \to z$
	$\dot{z} = a_1 z - \frac{1}{2}y^2 + a_2 z^2 + a_3$		
5	$\dot{x} = y$	No constraint	$z \to y$
	$\dot{y} = -x + yz$		$y \to z$
	$\dot{z} = a_1 z + \frac{1}{2}y^2 + a_2 z^2 + a_3$		

Table 2. Designed chaotic systems that have identical MSF in different coupling configurations.

Basic System	Equations	Function f		Couplings with Identical MSF
Sprott-A	$\dot{x} = y$ $\dot{y} = -x + yz$ $\dot{z} = f$	$f = x - 0.1y - 0.1z - 0.3y^2 + 0.2z^2 - 0.6yz + 2.5$	(14)	$z \to x$ $x \to y$
		$f = -\frac{1}{2}y^2 + 0.01z^2 + 1.2$	(15)	$z \to x$ $x \to z$
Sprott-B	$\dot{x} = yz$ $\dot{y} = x - y$ $\dot{z} = f$	$f = -0.16x + y + 0.08z^2 + 0.03$	(16)	$z \to y$ $y \to x$
Sprott-D	$\dot{x} = -y$ $\dot{y} = x + z$ $\dot{z} = f$	$f = 0.49x - 7 - 0.49x^2$	(17)	$x \to x$ $z \to z$
Jerk	$\dot{x} = y$ $\dot{y} = z$ $\dot{z} = f$	$f = -1.37x - 10.97y + 0.01x^2 + 0.52y^2 + 0.46$	(18)	$x \to y$ $y \to z$
		$f = 1.2x - 3.7y - 0.09x^2 - 0.42xy + 0.46$	(19)	$z \to z$ $y \to y$
Sprott-F	$\dot{x} = y + z$ $\dot{y} = -x + \alpha y$ $\dot{z} = f$	$f = 0.016y - 0.2x^2 + y^2 + z^2 + 2yz$ $\alpha = -0.016$	(20)	$x \to y$ $x \to z$
		$f = x + 0.38y + 0.5z + 0.005y^2 + 0.02z^2$ $+ 0.02yz - 2.3$ $\alpha = -0.26$	(21)	$z \to x$ $x \to y$
		$f = -x - 11.66z + 0.28z^2$ $\alpha = 0.12$	(22)	$z \to y$ $y \to z$
		$f = -x + 0.43y - 0.23z - 0.15y^2 + 5.78$ $\alpha = -0.23$	(23)	$y \to y$ $z \to z$
Sprott-G	$\dot{x} = \alpha x + z$ $\dot{y} = xz - y$ $\dot{z} = f$	$f = -5.71x + y + 1.64z - 0.5xz$ $\alpha = -1$	(24)	$z \to y$ $x \to z$
Sprott-O	$\dot{x} = y$ $\dot{y} = x - z$ $\dot{z} = f$	$f = 12.06y + 0.58z - 0.03z^2 + 0.53$	(25)	$y \to x$ $x \to y$

$$
\begin{aligned}
y \to y: &\quad \Lambda^3 + (-f_z + k - z)\Lambda^2 + (1 - f_z k - f_y y + f_z z)\Lambda - f_z - f_x y = 0,\\
z \to y: &\quad \Lambda^3 + (-f_z - z)\Lambda^2 + (1 + f_y k - f_y y + f_z z)\Lambda - f_z + f_x k - f_x y = 0,\\
x \to z: &\quad \Lambda^3 + (-f_z - z)\Lambda^2 + (1 - f_y y + f_z z)\Lambda - f_z - f_x y + k y = 0,\\
y \to z: &\quad \Lambda^3 + (-f_z - z)\Lambda^2 + (1 - f_y y + f_z z + k y)\Lambda - f_z - f_x y = 0,\\
z \to z: &\quad \Lambda^3 + (-f_z + k - z)\Lambda^2 + (1 - f_y y + f_z z - k z)\Lambda + k - f_z - f_x y = 0.
\end{aligned}
\tag{11}
$$

In order to have similar MSFs for any subset of the coupling configurations, their characteristic equations must be the same. Hence, f_x, f_y, and f_z are found to obey similar eigenvalues equations. For instance, the equations of two coupling configurations $y \to x$ and $z \to x$ are the same if,

$$
\begin{aligned}
f_x &= -1,\\
f_z + f_y &= y + z.
\end{aligned}
\tag{12}
$$

All the possible cases leading to similar MSFs for the system of Eq. (7) are given in Table 1.

Finally, the parameters of all the cases found (Table 1) for a chaotic solution are obtained with a systematic computer search. For example, one of the obtained systems that has the form of Case 2 in Table 1 with identical MSFs in $z \to x$ and $x \to y$ coupling configurations is defined as

$$
\begin{aligned}
\dot{x} &= y,\\
\dot{y} &= -x + yz,\\
\dot{z} &= x - 0.1y - 0.1z - 0.3y^2 + 0.2z^2\\
&\quad - 0.6yz + 2.5.
\end{aligned}
\tag{13}
$$

Using a similar procedure, the conditions are derived for the other mentioned basic chaotic systems. Subsequently, new chaotic systems are found with identical MSF curves in different coupling configurations. The designed chaotic systems and their parameters are given in Table 2.

3. Results

In the previous section, basic chaotic systems with identical MSFs in different coupling configurations

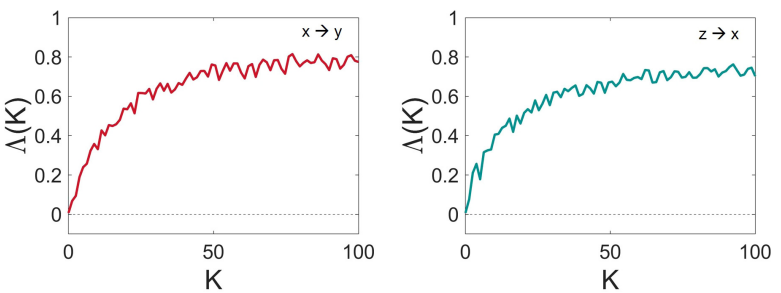

Fig. 3. Master stability functions ($\Lambda(K)$) for the Sprott-A system [Eq. (14)] in dependence on K for $x \to y$ and $z \to x$ couplings.

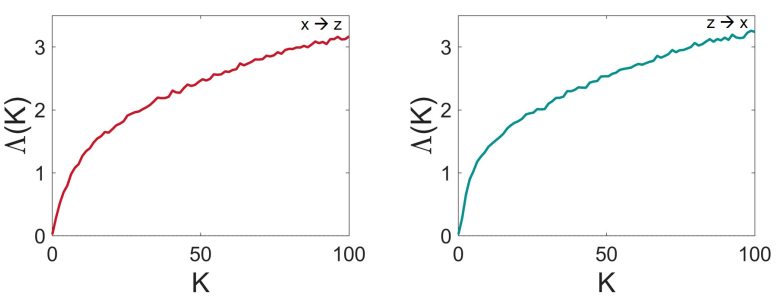

Fig. 4. Master stability functions ($\Lambda(K)$) for the Sprott-A system [Eq. (15)] in dependence on K for $x \to z$ and $z \to x$ couplings.

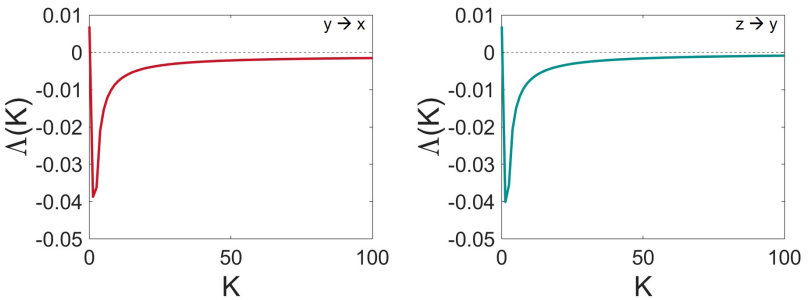

Fig. 5. Master stability functions ($\Lambda(K)$) for the Sprott-B system [Eq. (16)] in dependence on K for $y \to x$ and $z \to y$ couplings.

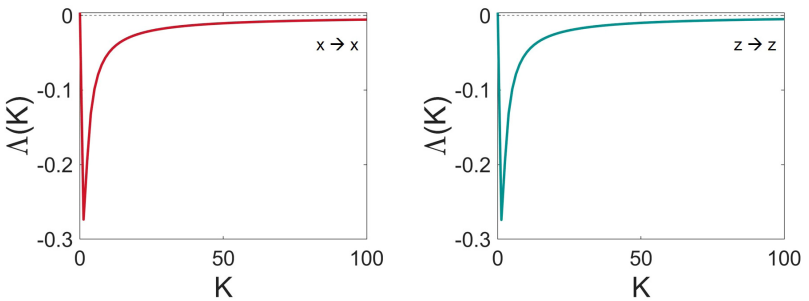

Fig. 6. MSFs ($\Lambda(K)$) for the Sprott-D system [Eq. (17)] in dependence on K for $x \to x$ and $z \to z$ couplings.

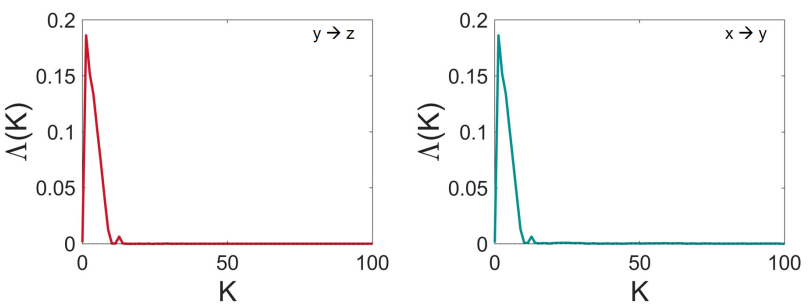

Fig. 7. Master stability functions ($\Lambda(K)$) for the Jerk system [Eq. (18)] in dependence on K for $y \to z$ and $x \to y$ couplings.

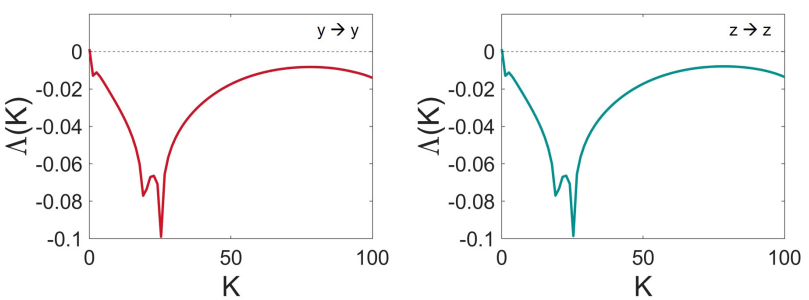

Fig. 8. Master stability functions ($\Lambda(K)$) for the Jerk system [Eq. (19)] in dependence on K for $y \to y$ and $z \to z$ couplings.

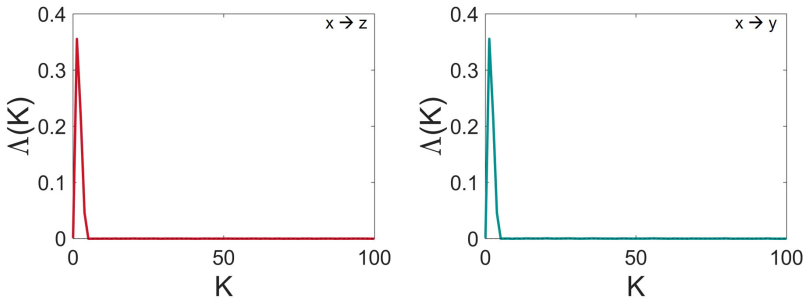

Fig. 9. Master stability functions ($\Lambda(K)$) for the Sprott-F system [Eq. (20)] in dependence on K for $x \to z$ and $x \to y$ couplings.

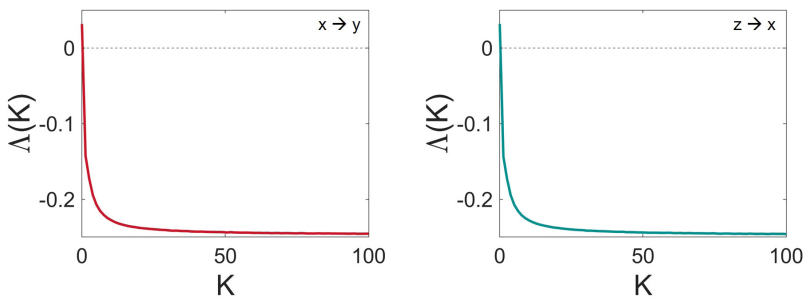

Fig. 10. Master stability functions ($\Lambda(K)$) for the Sprott-F system [Eq. (21)] in dependence on K for $x \to y$ and $z \to x$ couplings.

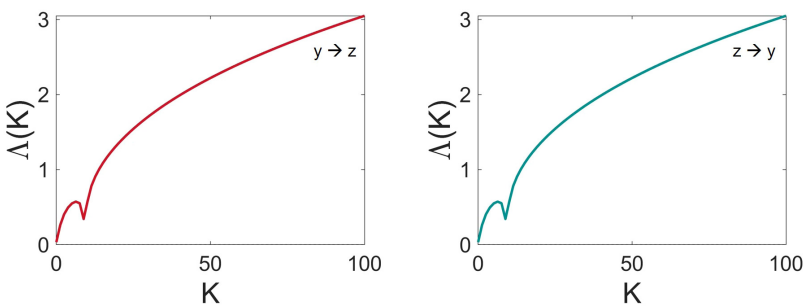

Fig. 11. Master stability functions ($\Lambda(K)$) for the Sprott-F system [Eq. (22)] in dependence on K for $y \to z$ and $z \to y$ couplings.

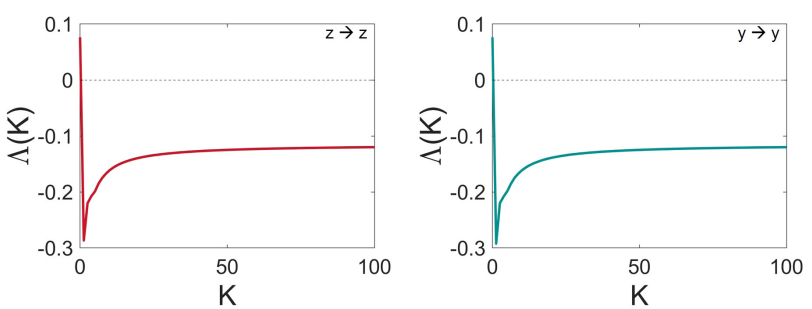

Fig. 12. MSFs ($\Lambda(K)$) for the Sprott-F system [Eq. (23)] in dependence on K for $z \to z$ and $y \to y$ couplings.

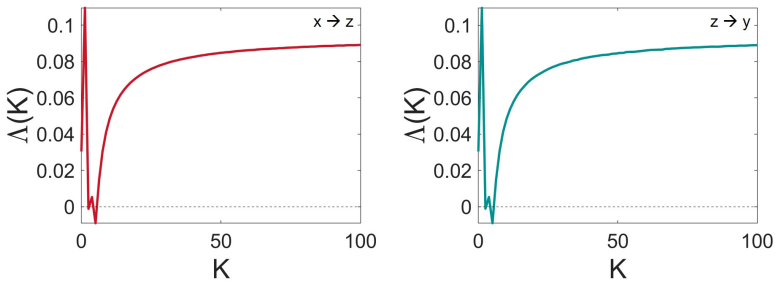

Fig. 13. Master stability functions ($\Lambda(K)$) for the Sprott-G system [Eq. (24)] in dependence on K for $x \to z$ and $z \to y$ couplings.

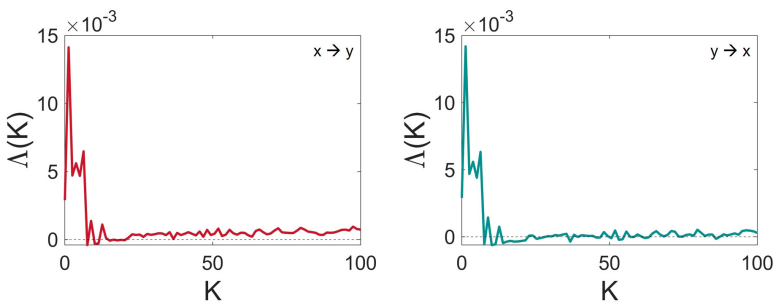

Fig. 14. Master stability functions ($\Lambda(K)$) for the Sprott-O system [Eq. (25)] in dependence on K for $x \to y$ and $y \to x$ couplings.

were found. In this section, the MSFs of those systems (Table 2) are found by numerically computing the maximum Lyapunov exponent of Eq. (A.3). Then, the apparently identical MSFs are plotted for two corresponding coupling configurations. The results are shown in Figs. 3 to 14. It can be seen that the method could successfully design the systems with similar MSF curves. However, in some cases there are some minor differences between the curves (for example in Fig. 3) which is related to the challenges of LLE simulations.

4. Conclusion

In this paper, some chaotic systems with equivalent synchronization patterns in different coupling configurations were constructed. The local stability of synchronization in coupled dynamical systems can be computed by the master stability function (MSF) method. Different coupling schemes can be constructed for linearly coupled oscillators depending on the variables involved in the coupling. The systems introduced here have equivalent MSFs in two different coupling configurations. Systems with similar MSF curves are rare. Earlier research has demonstrated that for various coupling schemes, circulant systems and special jerk systems have equivalent MSFs for some different couplings. Here, new chaotic systems with this feature were developed on the basis of basic chaotic systems. Some systems, such as generalized Sprott-A, Sprott-B, Sprott-D, Sprott-F, Sprott-G, Sprott-O, and a jerk system, were considered with a general polynomial form for their third equation. The prerequisites for equivalent MSFs in various coupling configurations were then inferred. These constraints defined the third equation of the systems under consideration. Subsequently, the parameters, which fulfill this aim, were found using a systematic computer search such that the defined system has a chaotic solution. Finally, 12 chaotic systems were found, and their identical MSFs were presented.

In terms of application, the importance of these systems may be having an alternative in the coupling function. If a functional coupling develops a problem, while the network is in operation or if using some of the variables in the coupling is not possible or practical, the coupling can be replaced with an equivalent alternative without affecting the network's performance.

Acknowledgment

This work is partially funded by Centre for Nonlinear Systems, Chennai Institute of Technology, India vide funding number CIT/CNS/2023/RP/012.

References

Amritkar, R. & Rangarajan, G. [2009] "Stability of multicluster synchronization," *Int. J. Bifurcation and Chaos* **19**, 4263–4271.

Antonik, P., Gulina, M., Pauwels, J. & Massar, S. [2018] "Using a reservoir computer to learn chaotic attractors, with applications to chaos synchronization and cryptography," *Phys. Rev. E* **98**, 012215.

Belykh, I., Hasler, M., Lauret, M. & Nijmeijer, H. [2005] "Synchronization and graph topology," *Int. J. Bifurcation and Chaos* **15**, 3423–3433.

Boccaletti, S., Kurths, J., Osipov, G., Valladares, D. & Zhou, C. [2002] "The synchronization of chaotic systems," *Phys. Rep.* **366**, 1–101.

Boccaletti, S., Latora, V., Moreno, Y., Chavez, M. & Hwang, D.-U. [2006] "Complex networks: Structure and dynamics," *Phys. Rep.* **424**, 175–308.

Chen, X., Huang, T., Cao, J., Park, J. H. & Qiu, J. [2019] "Finite-time multi-switching sliding mode synchronisation for multiple uncertain complex chaotic systems with network transmission mode," *IET Contr. Th. Appl.* **13**, 1246–1257.

Couzin, I. D. [2018] "Synchronization: The key to effective communication in animal collectives," *Trend. Cognit. Sci.* **22**, 844–846.

Dahms, T., Lehnert, J. & Schöll, E. [2012] "Cluster and group synchronization in delay-coupled networks," *Phys. Rev. E* **86**, 016202.

Faghani, Z., Wang, Z., Parastesh, F., Jafari, S. & Perc, M. [2020] "Is there a relation between synchronization stability and bifurcation type?" *Int. J. Bifurcation and Chaos* **30**, 2050123-1–8.

Franović, I., Todorović, K., Vasović, N. & Burić, N. [2012] "Cluster synchronization of spiking induced by noise and interaction delays in homogenous neuronal ensembles," *Chaos* **22**, 033147.

Franović, I., Todorović, K., Vasović, N. & Burić, N. [2014] "Stability, coherent spiking and synchronization in noisy excitable systems with coupling and internal delays," *Commun. Nonlin. Sci. Numer. Simul.* **19**, 3202–3219.

Frolov, N. & Hramov, A. [2021] "Extreme synchronization events in a Kuramoto model: The interplay between resource constraints and explosive transitions," *Chaos* **31**, 063103.

Li, Z. & Chen, G. [2006] "Global synchronization and asymptotic stability of complex dynamical networks," *IEEE Trans. Circuit. Syst.-II* **53**, 28–33.

Lü, J., Yu, X. & Chen, G. [2004] "Chaos synchronization of general complex dynamical networks," *Physica A* **334**, 281–302.

Moskalenko, O., Phrolov, N., Koronovskii, A. & Hramov, A. [2013] "Synchronization in the network of chaotic microwave oscillators," *Euro. Phys. J. Spec. Top.* **222**, 2571–2582.

Panahi, S., Nazarimehr, F., Jafari, S., Sprott, J. C., Perc, M. & Repnik, R. [2021] "Optimal synchronization of circulant and non-circulant oscillators," *Appl. Math. Comput.* **394**, 125830.

Parastesh, F., Mehrabbeik, M., Rajagopal, K., Jafari, S. & Perc, M. [2022] "Synchronization in Hindmarsh–Rose neurons subject to higher-order interactions," *Chaos* **32**, 013125.

Pecora, L. M. & Carroll, T. L. [1990] "Synchronization in chaotic systems," *Phys. Rev. Lett.* **64**, 821.

Pecora, L. M. & Carroll, T. L. [1998] "Master stability functions for synchronized coupled systems," *Phys. Rev. Lett.* **80**, 2109.

Pecora, L. M. & Carroll, T. L. [2015] "Synchronization of chaotic systems," *Chaos* **25**, 097611.

Pikovsky, A., Rosenblum, M. & Kurths, J. [2002] *Synchronization*: *A Universal Concept in Nonlinear Science* (American Association of Physics Teachers).

Rafikov, M. & Balthazar, J. M. [2008] "On control and synchronization in chaotic and hyperchaotic systems via linear feedback control," *Commun. Nonlin. Sci. Numer. Simul.* **13**, 1246–1255.

Rakshit, S., Bera, B. K. & Ghosh, D. [2018] "Synchronization in a temporal multiplex neuronal hypernetwork," *Phys. Rev. E* **98**, 032305.

Rakshit, S. & Ghosh, D. [2020] "Generalized synchronization on the onset of auxiliary system approach," *Chaos* **30**, 111102.

Rosenblum, M. G., Pikovsky, A. S. & Kurths, J. [1996] "Phase synchronization of chaotic oscillators," *Phys. Rev. Lett.* **76**, 1804.

Rosenblum, M. G., Pikovsky, A. S. & Kurths, J. [1997] "From phase to lag synchronization in coupled chaotic oscillators," *Phys. Rev. Lett.* **78**.

Sawicki, J., Hartmann, L., Bader, R. & Schöll, E. [2022] "Modelling the perception of music in brain network dynamics," *Front. Netw. Physiol.* **2**, 910920.

Sprott, J. C. [1994] "Some simple chaotic flows," *Phys. Rev. E* **50**, R647.

Tang, Y., Li, Q., Dong, W., Hu, M. & Zeng, R. [2021] "Optical chaotic communication using correlation demodulation between two synchronized chaos lasers," *Opt. Commun.* **498**, 127232.

Wang, Q., Perc, M., Duan, Z. & Chen, G. [2009] "Synchronization transitions on scale-free neuronal networks due to finite information transmission delays," *Phys. Rev. E* **80**, 026206.

Wang, Y., Lu, J., Liang, J., Cao, J. & Perc, M. [2018] "Pinning synchronization of nonlinear coupled Lur'e networks under hybrid impulses," *IEEE Trans. Circuits Syst.-II* **66**, 432–436.

Zhou, P., Yao, Z., Ma, J. & Zhu, Z. [2021] "A piezoelectric sensing neuron and resonance synchronization between auditory neurons under stimulus," *Chaos Solit. Fract.* **145**, 110751.

Appendix A
Master Stability Function

A network of coupled oscillators can be described as,

$$\dot{X}_i = F(X_i) - \sigma \sum_{j=1}^{N} L_{ij} H(X_j), \qquad \text{(A.1)}$$

where X_i is an m-dimensional state vector, F defines the local nonlinear oscillator dynamics, $i = 1, \ldots, N$ denotes the index of the network nodes, and σ shows the overall coupling strength. The $N \times N$ matrix L is the Laplacian matrix of the network, and H defines the coupling scheme, i.e. how the m-dimensional vectors are coupled into the system X_i. For a linear coupling $H(X) = hX$, where h is an $m \times m$ matrix with $h_{kl} = 1$ if the coupling is in $l \to k$ and $h_{kl} = 0$, else. Considering X_s as the synchronous solution, a small perturbation from the synchronization is denoted as $\delta X_i = X_i - X_s$ which obeys the linearized variational equations

$$\delta \dot{X}_i(t) = DF(X_s) - \sigma \sum_{j=1}^{N} L_{ij} DH(X_s) \delta X_j, \qquad \text{(A.2)}$$

where $DF(X_s)$ and $DH(X_s)$ denote the Jacobian of F and H, respectively, at the synchronous manifold for the linear diffusive coupling, $DH(X_s) = h$. The variational equations Eq. (A.2) can be decoupled by diagonalizing the Laplacian matrix L as

$$\dot{\eta}_i(t) = [DF(X_s) - \sigma \lambda_i h] \eta_i, \qquad \text{(A.3)}$$

where the m-dimensional vector η_i denotes the variations of the ith oscillator, $\lambda_i = 0, \lambda_2, \ldots, \lambda_N$ are the eigenvalues of the Laplacian matrix and $\boldsymbol{\eta} = Q^{-1} \boldsymbol{\delta} \mathbf{X} = (\eta_1, \ldots, \eta_N)$ is the Nm-dimensional vector of the transformed perturbations using the eigenvectors of $L(Q)$. For $\lambda_1 = 0$, the variational equation evolves along the synchronous manifold, and for the other eigenvalues, it evolves transverse to the synchronous manifold. The stability of the variational equation is obtained through computing its largest Lyapunov exponent (Λ) as a function of λ_i, known as MSF. In general, the rescaled coupling parameter $K = \sigma \lambda$ is considered, and Λ is found as a function of K. For K values with $\Lambda(K) < 0$, the variations asymptotically decay to zero leading to local stability of the synchronous manifold.